Effect of subband mixing on the energy levels of a hydrogenic impurity in a $GaAs/Ga_{1-x}Al_xAs$ double quantum well in a magnetic field

N. Nguyen, R. Ranganathan, B. D. McCombe, and M. L. Rustgi
Department of Physics and Astronomy, State University of New York at Buffalo, Buffalo, New York 14260
(Received 5 August 1991; revised manuscript received 13 December 1991)

In view of the recent evidence found in favor of subband mixing in coupling of confined impurity states in doped double-quantum-well structures, a variational approach employing Gaussian trial wave functions has been used to calculate the binding energies of the ground, ($1s$, $m=0$) and first excited, ($2p_-$, $m=-1$) states of a hydrogenic donor associated with the mixture of subbands of a double-GaAs quantum well coupled by a layer of $Ga_{1-x}Al_xAs$ in the presence of a magnetic field. Two different well sizes and three different locations of the impurity, (A) at the outer edge, (B) at the center, and (C) at the inner edge of the well, are considered, and the barrier width is allowed to vary. It is found that for the structures considered here the results from the calculations using the mixture of only first (symmetric) and second (asymmetric) subbands are significantly different from those using only the lowest (symmetric) subband, especially for the intermediate barrier widths, and depend strongly on the location of the impurity in the well. These results demonstrate that subband mixing should be included in double-quantum-well structure calculations. The effect of varying the magnetic field on the binding energies is also studied. A comparison with the measurements of Ranganathan *et al.* [Phys. Rev. B **44**, 1423 (1991)] demonstrates that the agreement is not improved when mixing of subbands higher than the lowest two is included in the calculation.

I. INTRODUCTION

In recent years, the development of superlattice structures using crystal-growth techniques, such as molecular-beam epitaxy and metal-organic chemical-vapor deposition, has led to the discovery and exploration of new phenomena[1–5] and applications. The latter include infrared detectors, resonant tunneling diodes, and ballistic transistors.

There have been a number of studies of the electronic properties of shallow donors in quantum wells.[6–10] The observations of Jarosik *et al.*[11] are in good agreement with the calculations of Greene and Bajaj[6] for the $1s-2p_-$ and $1s-2p_+$ transitions (usual hydrogen-atom notation) of the on-center hydrogenic donor in a $GaAs/Ga_{0.75}Al_{0.25}As$ single quantum well in the presence of a magnetic field.[12] Studies of the effects of finite barrier widths on the impurity states have been made by others. Chaudhuri[7] calculated the binding energy of a hydrogenic impurity in a $GaAs/Ga_{1-x}Al_xAs$ three-quantum-well structure which is valid for small barrier height and/or thin barriers. Lane and Green[8] have included effects of finite barrier widths in multiple-quantum-well structures. Chen and Zhou[10] dealt with a double-quantum-well structure in the absence of a magnetic field. In these calculations, carried out in the envelope-function approximation, no account was taken of mixing of the different confinement state wave functions by the impurity potential; namely, only the ground subband envelope function was used in the trial wave function. However, recent calculations of Nguyen *et al.*[13] and their comparison with the observations of Ranganathan *et al.*[14] point to the need to include subband mixing[15] in such calculations.

In order to determine the range of well and barrier parameters over which such confinement subband mixing is important in coupled double wells, calculations including mixing of the lowest two subbands are reported for two different well sizes ($L=50$ and 170 Å) and three different locations of the impurity: (A) at the outer edge, (B) on center, and (C) at the inner edge of the well. The effects of varying the barrier width and the magnetic field are also studied for these structures. The validity of these calculations is also tested by inclusion of higher subband mixing.

II. METHOD OF CALCULATION

A schematic diagram of the double-quantum-well structure with three different locations of the impurity is shown in Fig. 1. The symmetric double quantum well consists of two GaAs wells of thickness L coupled by a $Ga_{1-x}Al_xAs$ barrier of thickness W. A uniform magnetic field is considered parallel to the growth axis, perpendicular to the interfaces between the wells and barriers.

In the framework of the effective-mass approximation, the Hamiltonian for the electron is given by

$$H=\frac{m^*}{m_e^*}\left[-\nabla^2+\gamma L_z+\frac{\gamma^2\rho^2}{4}\right]-\frac{2}{r}+V(z)\ . \qquad (1)$$

Atomic units in GaAs have been employed; all distances are in units of the effective Bohr radius $a_0=\hbar^2\epsilon_0/m^*e^2=98.7$ Å; all energies are in units of the effective Rydberg $R=m^*e^4/2\hbar^2\epsilon_0^2=5.83$ meV, and the dimensionless measure of the magnetic field is defined as

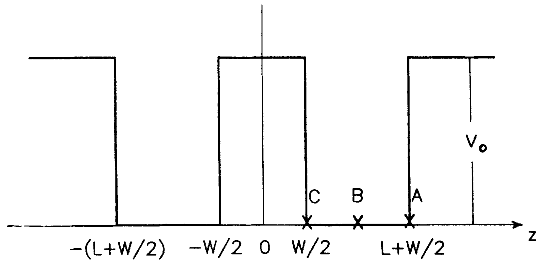

FIG. 1. Schematic illustration of the double-quantum-well structure in a magnetic field. The ×'s labeled (A), (B), and (C) indicate the three positions of the donor ion considered: (A) the outer edge, (B) on center, and (C) the inner edge of well.

$\gamma = e\hbar B/2m^*cR$, where m^* and ϵ_0 are the electronic effective mass and dielectric constant of GaAs, respectively. In Eq. (1), m_e^* is the effective mass of an electron, which is different in the two semiconductors, and the static dielectric constant is assumed to be the same everywhere. The origin of the cylindrical coordinates is chosen to be at the center of the central barrier, and the electronic position $r=[\rho^2+(z-z_I)^2]^{1/2}$, where z_I is the position of the impurity atom, and ρ is the distance in the x-y plane. The z component of the angular-momentum operator in units of $\hbar$ is L_z. The barrier potential is

$$V(z)=\begin{cases} 0, & \dfrac{W}{2}<|z|<L+\dfrac{W}{2} \\ V_0, & \dfrac{W}{2}>|z| \text{ and } |z|>\dfrac{W}{2}+L\ . \end{cases} \tag{2}$$

A variational approach is used to calculate the eigenvalues of the Hamiltonian. The trial electronic wave function that includes mixing of the subband states is chosen to be

$$\psi(\rho,z,\phi)=G(\rho,z-z_I,\phi)\sum_{n=1}^{N} a_n f_n(z)\ , \tag{3}$$

where the summation is taken over the states of a free electron in the one-dimensional double square well with the potential $V(z)$. The functions $f_n(z)$ are given by

$$f_n(z)=\begin{cases} A_n e^{\kappa_n z}, & z<-\left[L+\dfrac{W}{2}\right] \\ B_n\cos(k_n z)+C_n\sin(k_n z), & -\left[L+\dfrac{W}{2}\right]<z<-\dfrac{W}{2} \\ D_n e^{\kappa_n z}+E_n e^{-\kappa_n z}, & -\dfrac{W}{2}<z<\dfrac{W}{2} \\ F_n\cos(k_n z)+G_n\sin(k_n z), & \dfrac{W}{2}<z<L+\dfrac{W}{2} \\ H_n e^{-\kappa_n z}, & L+\dfrac{W}{2}<z\ , \end{cases} \tag{4}$$

the coefficients a_n are variational parameters subject to the normalization constraint

$$\sum_{n=1}^{N}|a_n|^2=1\ , \tag{5}$$

and N is chosen such that the inclusion of subbands higher than N does not change the numerical results. In our calculations, only the two lowest bands ($N=2$) were needed as the results were found to be insensitive to the inclusion of higher subbands.

The wave number k_n is determined from the energy of the subband, and by assuming that $f_n(z)$ and $(1/m_e^*)df_n/dz$ (Ref. 16) are continuous across the interfaces, κ_n and other coefficients are determined.

The Hamiltonian has cylindrical symmetry which ensures that the ϕ dependence of the wave function has the form $e^{im\phi}$, where m is the quantum number associated with the angular momentum in the z direction. The function $G(\rho,z-z_I,\phi)$ can be written as

$$G(\rho,z-z_I,\phi)=\rho^{|m|}e^{im\phi}\sum_{i,j}A_{ij}G_{ij}(\rho,z-z_I)\ . \tag{6}$$

The basis functions $G_{ij}(\rho,z-z_I)$ are Gaussians in ρ and z variables

$$G_{ij}(\rho,z-z_I)=e^{-\alpha_i(z-z_I)^2}e^{-(\alpha_j+\beta)\rho^2}\ , \tag{7}$$

where β and A_{ij} are variational parameters. Since the symmetry of our structure is similar to that of Ref. 6 which gives good agreement with experiments for both symmetric (on-center) impurity and asymmetric (inner-edge or outer-edge impurity) cases,[11,17] the set of parameters α_i is taken from Table I of Ref. 6. The number of basis functions is restricted by requiring $A_{ij}=0$ for $|i-j|>1$ which gives 13 and 10 basis functions, respectively, for the ground ($m=0$) and first ($m=-1$) excited states. The eigenvalues E_1 $(m=0)$ and E_2 $(m=-1)$ are determined by numerically minimizing $\langle\psi|H|\psi\rangle/\langle\psi|\psi\rangle$.

The binding energies for the ground $(E_{1s}, m=0)$ and first $(E_{2p_-}, m=-1)$ excited states are

$$E_{1s}=E_0+\gamma-E_1 ,\quad E_{2p_-}=E_0+\gamma-E_2 , \tag{8}$$

where E_0 is the lowest energy of a free electron in the potential given by Eq. (2), and γ is the energy of the lowest Landau level. The binding energy of the second excited state $(2p_+, m=1)$ is given by

$$E_{2p_+}=E_{2p_-}+2\gamma , \tag{9}$$

where 2γ is the cyclotron energy.

The calculations have been done for $V_0=230$ meV, which is about 60% of the band-gap difference between GaAs and $Ga_{0.7}Al_{0.3}As$. The electronic effective mass is determined from the expression[6]

$$m_e^*=(0.067+0.083x)m_e , \tag{10}$$

where m_e is the rest mass of the electron and x is the Al concentration. Thus for GaAs, $m_e^*=0.067m_e$ and for $Ga_{0.7}Al_{0.3}As$, $m_e^*=0.0919m_e$. The effect of a heavier mass in $Ga_{0.7}Al_{0.3}As$ is taken into account in matching the continuity of $(m^*/m_e^*)\partial f/\partial z$ at the interface and leads to a slight increase in the zero-field binding energy by comparison to the condition $\partial f/\partial z$ continuous because the electron wave function is more confined in the well.

III. RESULTS AND DISCUSSION

In order to compare the results of the calculations with and without considering subband mixing, the calculated energies of the ground $(1s)$ and first excited $(2p_-)$ states under the two different conditions are plotted for $B=6.75$ T, which corresponds to $\gamma=1$, as functions of barrier width in Figs. 2 and 3 for well sizes of 50 and 170 Å, and three different locations of the impurity: (A) at the outer edge, (B) on center, and (C) at the inner edge of the well. In both of these figures the solid and the dotted curves display the results of the calculations for all cases, with and without mixing, respectively. In both Figs. 2 and 3, for zero barrier width, the binding energy corresponds to a single well of twice the well size considered in the calculation, with the impurity at the corner [for (A)], one-fourth away from the center [for (B)], or at the center [for (C)] of the well; for the limit of infinite barrier width,

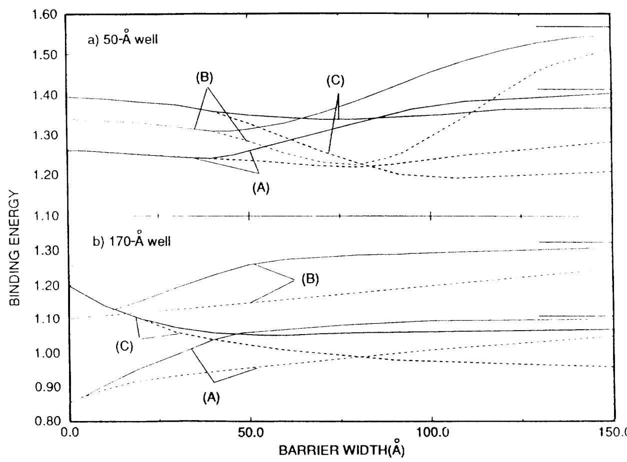

FIG. 3. Binding energy (in units of R) of the $2p_-$ state. For other details, see Fig. 2.

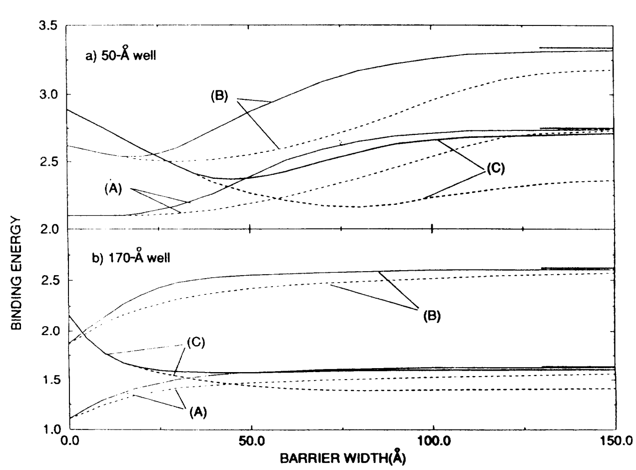

FIG. 2. Binding energy (in units of R) of the $1s$ state as function of barrier width for the (a) 50-Å and (b) 170-Å wells in a magnetic field of 6.75 T ($\gamma=1$) for the three locations of the impurity: (A) outer edge, (B) on center, and (C) inner edge of the well. The solid and dotted curves display the results for the calculations with and without mixing, respectively.

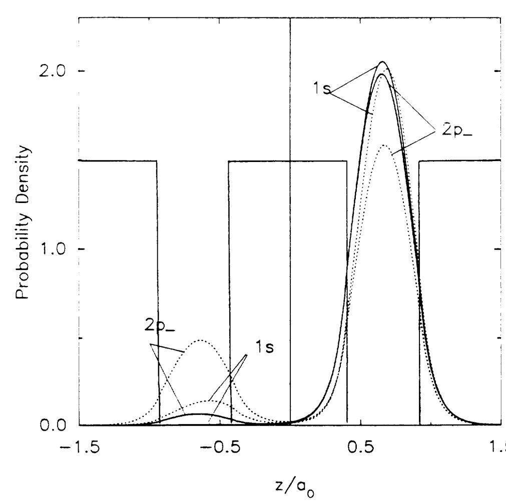

FIG. 4. Probability density of the donor electron in the $1s$ and $2p_-$ states as a function of *z expressed in units of the effective Bohr radius* a_0 for the outer edge (A) location of the impurity, for a 50-Å well and 80-Å barrier width in a magnetic field of 6.75 T. The solid and dashed curves display the results for the calculations with and without mixing, respectively.

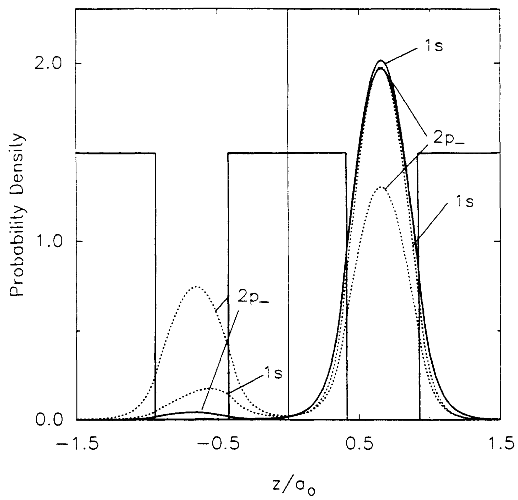

FIG. 5. Same as Fig. 4 but for the on-center (B) location of the impurity.

the binding energy is represented by the horizontal line which corresponds to that of a single well of the size considered here with the impurity ion at the center [for (B)] or edge [for (A) and (C)]. These single-well limits are calculated without inclusion of subband mixing since the energy separation between the lowest two subbands is large in these cases.

The results show (Figs. 2 and 3) that in all cases, and especially for the intermediate barrier width, with subband mixing the calculated energy is significantly larger than that without mixing (see Table I). These results are, however, sensitive only to the mixing of the two lowest subbands and insensitive to the inclusion of higher subbands (see Table II for the small effect of the higher subbands) because of the large energy separation between the second and higher subbands. Consequently, only the two lowest subbands were included for calculation throughout this paper. The variation of the binding ener-

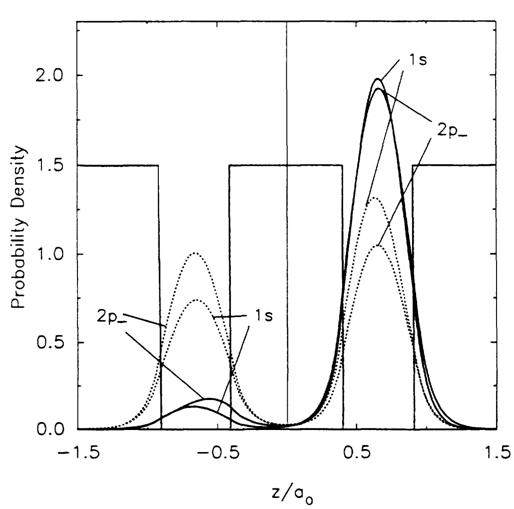

FIG. 6. Same as Fig. 5 but for the at inner-edge (C) location of the impurity.

TABLE I. Probability of the donor electron without (a) and with (b) subband mixing in the well containing the impurity for several barrier widths and three different locations: [at the outer edge (A), on center (B), and at the inner edge (C)] of the impurity.

Barrier width (Å)	(A)				(B)				(C)			
	1s		$2p_-$		1s		$2p_-$		1s		$2p_-$	
	(a)	(b)	(a)	(b)	(a)	(b)	(a)	(b)	(a)	(b)	(a)	(b)
					Well size $L=50$ Å							
20	0.493	0.496	0.427	0.429	0.479	0.488	0.416	0.417	0.418	0.427	0.403	0.413
40	0.583	0.690	0.452	0.476	0.576	0.718	0.433	0.470	0.439	0.598	0.404	0.416
80	0.781	0.826	0.594	0.798	0.792	0.823	0.518	0.801	0.564	0.832	0.419	0.770
150	0.825	0.826	0.800	0.827	0.814	0.823	0.764	0.818	0.811	0.832	0.654	0.827
					Well size $L=170$ Å							
5	0.737	0.751	0.619	0.631	0.796	0.854	0.604	0.637	0.496	0.506	0.492	0.494
9	0.791	0.826	0.657	0.690	0.835	0.904	0.636	0.702	0.497	0.524	0.494	0.502
18	0.866	0.935	0.734	0.838	0.912	0.959	0.730	0.831	0.507	0.618	0.495	0.540
30	0.917	0.974	0.794	0.934	0.951	0.981	0.801	0.939	0.519	0.823	0.501	0.666
48	0.946	0.985	0.860	0.984	0.973	0.986	0.853	0.980	0.547	0.970	0.509	0.924
150	0.964	0.985	0.985	0.985	0.990	0.987	0.972	0.985	0.840	0.984	0.654	0.985

TABLE II. Probability of the donor electron a_n^2 [see Eq. (3) for definition] on mixing two or more subbands for three different locations of the impurity: at the outer edge (A), on center (B), and at the inner edge (C). The corresponding binding energies (in Ry) are also given. (a) 50-Å well–40-Å barrier width. (b) 170-Å well–30-Å barrier width.

Number of mixing subbands	(A)				(B)				(C)			
	1s		$2p_-$		1s		$2p_-$		1s		$2p_-$	
	2	3	2	3	2	3	2	3	2	3	2	3
						(a)						
a_1^2	0.851	0.851	0.999	0.999	0.800	0.800	0.999	0.999	0.943	0.943	1.0	1.0
a_2^2	0.149	0.149	0.001	0.001	0.200	0.200	0.001	0.001	0.057	0.057	$\sim 10^{-4}$	$\sim 10^{-5}$
a_3^2		$\sim 10^{-8}$		$\sim 10^{-8}$		$\sim 10^{-6}$		$\sim 10^{-7}$		$\sim 10^{-4}$		$\sim 10^{-5}$
Energy	2.265	2.265	1.245	1.245	2.754	2.755	1.310	1.310	2.431	2.437	1.336	1.336
Number of mixing subbands	2	4	2	4	2	4	2	4	2	4	2	4
						(b)						
a_1^2	0.698	0.712	0.714	0.714	0.570	0.573	0.715	0.722	0.878	0.880	0.969	0.969
a_2^2	0.302	0.287	0.286	0.286	0.430	0.426	0.285	0.278	0.122	0.057	0.031	0.031
a_3^2		0.001		$\sim 10^{-4}$		$\sim 10^{-4}$		$\sim 10^{-4}$		0.057		$\sim 10^{-6}$
a_4^2		$\sim 10^{-4}$		$\sim 10^{-5}$		$\sim 10^{-4}$		$\sim 10^{-5}$		0.006		$\sim 10^{-6}$
Energy	1.516	1.516	1.002	1.002	2.443	2.444	1.211	1.212	1.594	1.602	1.073	1.073

gy due to mixing can be explained as follows. The mixing of the lowest symmetric and antisymmetric subbands confines the electron more in the well containing the impurity ion than without the mixing. This additional confinement increases the (negative) Coulomb potential energy and thus raises the binding energy. On the other hand, the inclusion of the higher subband raises the kinetic energy which results in a lowering of the binding energy. The optimum tradeoff is determined by the variational calculation. In the limit of small barrier width, the mixing is small because of the large energy splitting between the symmetric and antisymmetric confinement states. As the barrier width increases the splitting decreases, the mixing begins to be significant. This leads to increased binding energy as compared with the results obtained without mixing. For the 50-Å well significant mixing starts at a barrier width of about 20 Å; for the 170-Å well it starts at a much smaller barrier width because of its smaller energy splitting in comparison with the 50-Å well. In the same manner, the mixing increases as the barrier width increases until the two subbands are almost degenerate, then equal proportions of the symmetric and antisymmetric subbands are mixed. In the limit of large barrier width, although the mixing is large, the binding energy does not change much because without mixing the electron is already well confined in one well. The probability of the electron being in the well containing the donor for both situations, with and without mixing, is shown in Table I for several barrier widths. The probability density of the donor electron as a function of z with $\gamma=1$ is shown in Figs. 4–6. In general, except for the limits of very small and very large barrier widths, subband mixing does raise the binding energy. It is also observed that intersubband mixing depends upon the location of the impurity—the greater the asymmetric position of the impurity with respect to the center of the barrier, the smaller is the barrier width for which the mixing begins to become significant as the lack of orthogonality of the states increases with asymmetry.

The minima for some of the curves for the no-mixing case, as explained in Ref. 13, result from the interplay between two competing effects when the barrier width is increased: one effect is due to the spreading of the wave function into the wider barrier, which reduces the binding energy; the other is the increase of the confinement of the electron in one well which increases the binding energy. Since the effects of coupling on the impurity wave function are much reduced when subband mixing is considered, these minima are much less pronounced and are shifted to smaller values of the barrier width if they are noticeable at all.

Figures 7–9 display the binding energy as functions of the applied magnetic field for the three different positions of the impurity (A, B, and C) in the well, respectively. The results show that the binding energy increases as the magnetic field increases because the electron is more confined in the x-y plane due to application of the magnetic field. This reduces the positive magnetic term which is propositional to ρ^2 in Eq. (1) for the Hamiltonian, thus increasing the binding energy.

Figure 10 shows a comparison of our calculations with the measurements of Ref. 14 when intersubband mixing and the difference in the masses in the well and the barrier are taken into account. As before,[13] the quality of the agreement is not changed when the mixing of subbands higher than the lowest two is included, as is obvious from Table II.

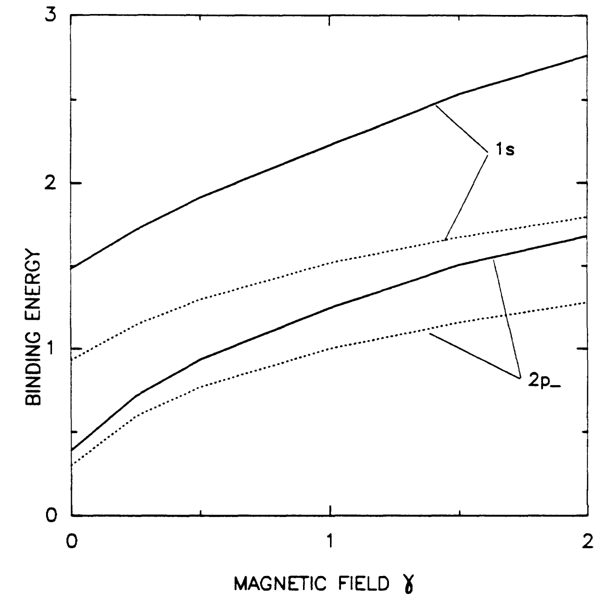

FIG. 7. Binding energies (in units of R) of the 1s and 2p_- states as functions of the applied magnetic field oriented normal to the wells ($\gamma=1$ corresponds to $B=6.75$ T) employing the subband mixing for the outer-edge (A) location of the impurity. The solid and dashed curves display the results for the 50-Å well–40-Å barrier width and 170-Å well–30-Å barrier width, respectively.

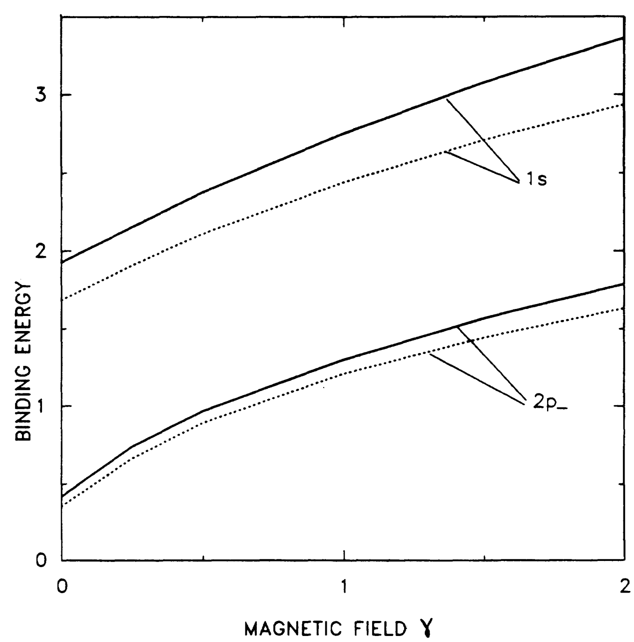

FIG. 8. Same as Fig. 7 but for the on-center (B) location of the impurity.

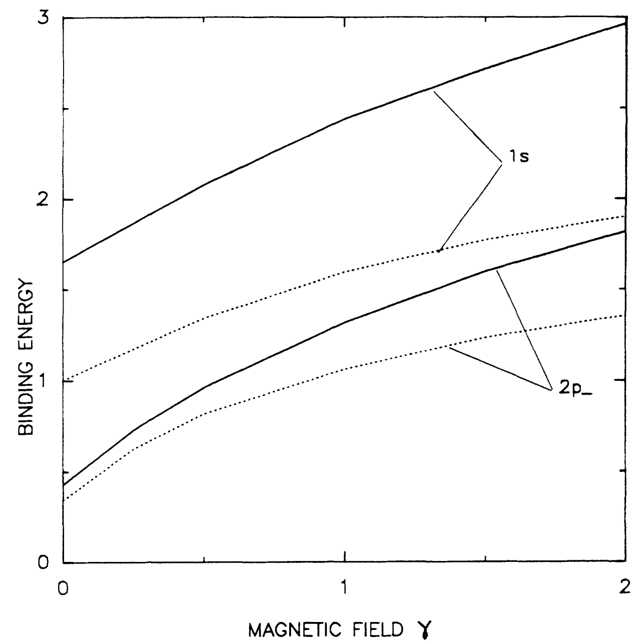

FIG. 9. Same as Fig. 7 but for the inner-edge (C) location of the impurity.

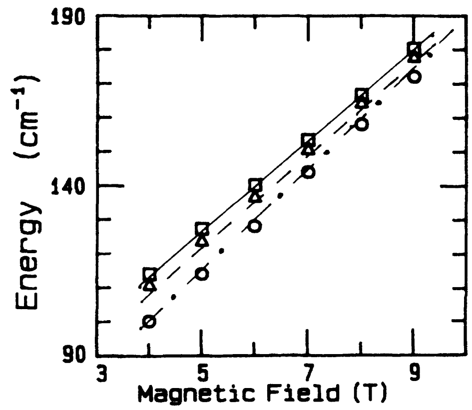

FIG. 10. The measured (data taken from Ref. 14 and denoted by symbols) and calculated (lines) hydrogenic donor transition energies vs magnetic field for the 170-Å-wide wells separated by a barrier of width 48 Å (solid, □), 18 Å (dashed, △), 9 Å (dotted-dashed, ○), respectively. The theoretical curves are obtained on considering intersubband mixing and the boundary condition of continuity of $(1/m_e^*)\,df/dz$.

In conclusion, our results show that intersubband mixing is important for calculations of the electronic binding energy of a hydrogenic impurity in a double square well, especially for intermediate width barriers. It is also observed that intersubband mixing depends upon the location of the impurity—the greater the asymmetric position of the impurity with respect to the center of the barrier, the smaller is the barrier width for which the mixing begins to become significant. Subband mixing may also play an important role in calculations of the energy levels of a hydrogenic impurity in multiple-quantum-well structures or in superlattices. The magnetic field is found to increase the binding energy of the donor electron in comparison with its value in a zero magnetic field as is the case for isolated wells.

ACKNOWLEDGMENT

One of the authors (M.L.R.) is grateful to Dr. D. J. Nagel of the Naval Research Laboratory for providing the facilities to carry out a part of this work. The work of two of us (R.R. and B.D.M.) was supported in part by ONR and by ONR/SDIO under the MFEL program.

[1]D. A. B. Miller, S. S. Chemla, T. C. Damen, A. C. Gossard, W. Wiegmann, T. H. Wood, and C. A. Burrus, Phys. Rev. Lett. **53**, 2173 (1984).

[2]T. C. L. G. Sollner, W. D. Goodhue, P. E. Tannenwald, C. D. Parker, and D. O. Peck, Appl. Phys. Lett. **43**, 588 (1983).

[3]E. Brown, W. D. Goodhue, and T. C. L. G. Sollner, J. Appl. Phys. **64**, 1519 (1988).

[4]B. F. Levine, C. G. Bethea, G. Hasnain, J. Walker, and R. J. Malik, Appl. Phys. Lett. **53**, 296 (1988).

[5]F. Capasso and R. A. Kiehl, J. Appl. Phys. **58**, 1366 (1985).

[6]R. L. Greene and K. K. Bajaj, Phys. Rev. B **31**, 913 (1985). References to earlier publications are contained in this paper.

[7]S. Chaudhuri, Phys. Rev. B **28**, 4480 (1983).

[8]R. L. Greene, and P. Lane, Phys. Rev. B **34**, 8639 (1986); P. Lane and R. L. Greene, *ibid.* **33**, 5871 (1986).

[9]Z. Liu and D. Ma, J. Phys. C **19**, 2375 (1986).

[10]H. Chen and S. Zhou, Phys. Rev. B **36**, 9581 (1987).

[11]N. C. Jarosik, B. D. McCombe, B. V. Shannabrook, J. Comas, J. Ralston, and G. Wicks, Phys. Rev. Lett. **54**, 1283 (1985).

[12]J. P. Cheng and B. D. McCombe, Phys. Rev. B **42**, 7626 (1990).

[13]N. Nguyen, R. Ranganathan, B. D. McCombe, and M. L. Rustgi, Phys. Rev. B **44**, 3344 (1991).

[14]R. Ranganathan, B. D. McCombe, N. Nguyen, Y. Zhang, M. L. Rustgi, and W. J. Schaff, Phys. Rev. B **44**, 1423 (1991).

[15]I. Galbraith and G. Duggan, Phys. Rev. B **40**, 5515 (1989).

[16]G. Bastard, Phys. Rev. B **24**, 5693 (1981).

[17]J. M. Mercy, B. D. McCombe, W. Beard, J. Ralston, and G. Wicks, Surf. Sci. **196**, 334 (1988).